Accepted Manuscript

Efficient greenish-blue phosphorescent iridium(III) complexes containing carbene and triazole chromophores for organic light-emitting diodes

Hong Li, Yong-Ming Yin, Hong-Tao Cao, Hai-Zhu Sun, Li Wang, Guo-Gang Shan, Dong-Xia Zhu, Zhong-Min Su, Wen-Fa Xie

PII: S0022-328X(13)00848-6

DOI: 10.1016/j.jorganchem.2013.11.036

Reference: JOM 18381

To appear in: *Journal of Organometallic Chemistry*

Received Date: 28 October 2013

Revised Date: 24 November 2013

Accepted Date: 26 November 2013

Please cite this article as: H. Li, Y.-M. Yin, H.-T. Cao, H.-Z. Sun, L. Wang, G.-G. Shan, D.-X. Zhu, Z.-M. Su, W.-F. Xie, Efficient greenish-blue phosphorescent iridium(III) complexes containing carbene and triazole chromophores for organic light-emitting diodes, *Journal of Organometallic Chemistry* (2014), doi: 10.1016/j.jorganchem.2013.11.036.

Two iridium(III) complexes containing carbene-based cyclometalated ligands and pyridine-triazole ancillary ligand exhibit intense greenish-blue phosphorescent emission. The greenish-blue and white OLEDs using the titled complexes as the dopant emitters show effective electroluminescence efficiencies.

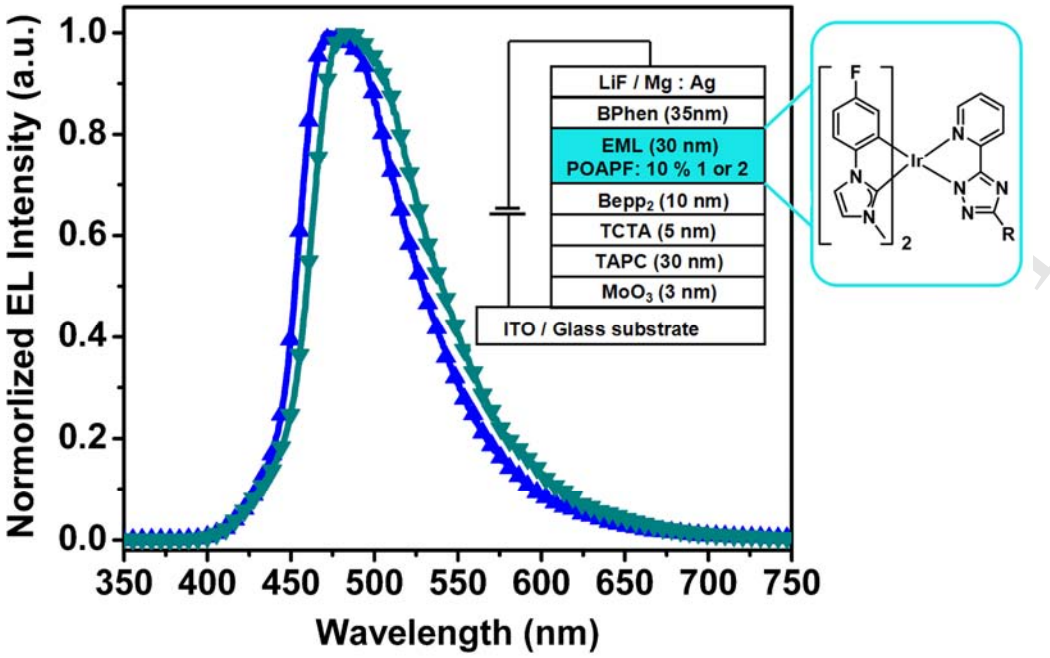

Efficient greenish-blue phosphorescent iridium(III) complexes containing carbene and triazole chromophores for organic light-emitting diodes

Hong Li[a], Yong-Ming Yin[b], Hong-Tao Cao[a], Hai-Zhu Sun[a], Li Wang[a], Guo-Gang Shan[a,] *, Dong-Xia Zhu[a], Zhong-Min Su[a,] *, Wen-Fa Xie[b,] *

[a]Institute of Functional Material Chemistry, Department of Chemistry, Northeast Normal University, Changchun, 130024, People's Republic of China

[b]State Key Laboratory on Integrated Optoelectronics, College of Electronic Science and Engineering, Jilin University, Changchun, 130012, People's Republic of China

*Corresponding author: Fax: +86-431-85684009; Tel.: +86-431-85099108.

E-mail: shangg187@nenu.edu.cn (G. G. Shan); zmsu@nenu.edu.cn (Z. M. Su)

*Corresponding author:

E-mail: xiewf@jlu.edu.cn (W. F. Xie).

Abstract

Two heteroleptic iridium(III) complexes using carbene as cyclometalated ligands and pyridine-triazole as ancillary ligand, namely **(fpmi)$_2$Ir(mtzpy)** (**1**) and **(fpmi)$_2$Ir(phtzpy)** (**2**) [**fpmi** = 1-(4-fluorophenyl)-3-methylimdazolin-2-ylidene-C,C$^{2'}$, **mtzpy** = 2-(5-methyl-2*H*-1,2,4-triazol-3-yl)pyridine, **phtzpy** = 2-(5-phenyl-2*H*-1,2,4-triazol-3-yl)pyridine], were synthesized and their structural, photophysical and electrochemical properties investigated systematically. Both complexes exhibit bright greenish-blue phosphorescence (λ_{max} ~490 nm) with quantum yields of about 0.50. Comprehensive density functional theory (DFT) approach was then performed to gain insights into their photophysical and electrochemical characters. The fabrication of organic light-emitting diodes (OLEDs), employing complexes **1** and **2** as phosphorescent dopants, was successfully achieved. Among them, the device based on **1** exhibited considerable power efficiency (η_p) of 11.43 lm W^{-1} and current efficiency (η_c) of 11.78 cd A^{-1}. With the merit of intrinsic characteristic of complex **1**, a white OLED comprised of **1** and one orange phosphor **(pbi)$_2$Ir(biq)** achieved a peak η_p of 9.95 lm W^{-1} and η_c of 10.81 cd A^{-1}, together with Commission Internationale de l'Eclairage (CIE) coordinates of (0.34, 0.40). The results indicate that two iridium(III) complexes reported here are promising phosphorescent dyes for OLEDs.

Keywords: Iridium(III) complex; Carbene; Triazole-pyridine; Greenish-blue emission; Organic light-emitting diode; Density functional theory

1. Introduction

Solid-state luminescent materials have attracted great attention due to their enormous potential applications in organic light-emitting diodes (OLEDs) and other optoelectronic material technology [1–7]. In OLEDs, recombination of electrons and holes in emitting layer gives rise to the formation of 25% singlet excitons and 75% triplet ones. For conventional fluorescent OLEDs, however, the 75% triplet excitons are usually lost due to the forbidden transition from the triplet to the ground state during electroluminescence process. To achieve high electroluminescence efficiency, efficient luminescent materials that can harness both singlet excitons and the spin-forbidden triplet excitons are highly desired. Since the pioneering electrophosphorescence works of Forrest and Ma et al. in 1998 [8, 9], intensive efforts have been carried out to design and synthesize phosphorescent materials for highly efficient OLEDs. The readily available, Ru(II)- [10–13], Os(II)- [14–15], Cu(I)- [16–19], Pt(II)- [18, 20–27] and Ir(III)- [28–40] based phosphorescent complexes can give effective harvesting of both singlet and triplet excitons endowed by heavy-atom spin-orbit coupling (SOC), achieving nearly 100% internal quantum efficiencies in theory [1, 8, 41]. In particular, iridium(III) complexes displaying high quantum yields, broad range of emission colors, excellent optical- and thermal- stabilities, as well as short excited-state lifetimes have been regarded as appealing phosphors for optical devices [4, 34]. To date, efficient red- and green- emitting iridium(III) complexes have been well developed through ingenious ligands modification [18, 42–44]. Despite these advances in display technology, the development of stable

phosphorescent materials with wide band gap, which is essential for solid-state lighting and flat panel displays, remains elusive and still challenge [45–50].

The above urgency prompts scientific researchers to develop appropriate design strategy for iridium(III) complexes with wide band gaps. In this respect, a number of intensive studies [4, 51] have been performed to obtain blue or greenish-blue materials by structural modification. The general approaches [18] to achieving such phosphorescent iridium(III) complexes can be mainly divided into following sections: i) introduction of electron-withdrawing groups on the phenyl rings of 2-phenylpyridine (ppy) type ligand such as fluorine, trifluoromethyl and cyanide, to stabilize the HOMO energy level of the complexes [52–54]; ii) addition of electron-donating groups to pyridine ring of ppy ligand, for instance methoxy and methylamine, to increase the LUMO energy level [55, 56]; iii) using N-heterocyclic ligand to replace pyridine ring to a higher LUMO, such as five membered heterocycle pyrazole or trizole [57, 58]. Although widened energy gap E_g can be obtained using the methods mentioned above, a mixture of the ligand centered π-π* and metal-to-ligand change transfer (MLCT) transitions may be found to gradually reduce, leading to a relatively low quantum yield.

It is well known that N-heterocyclic carbenes (NHCs) have been widely used in transition metal catalysts [59, 60]. Recently, the transition metal complexes containing NHCs moieties have been proved to be promising luminescent materials for OLEDs. Since they possess sufficiently large covalent metal-carbene bonds that are beneficial to stabilize the complexes [22, 61–70]. Furthermore, the strong ligand field of the

carbene can effectively further push up the energy of nonradiative d-d excited states on the metal center, resulting in stable phosphors with wide band gap and high quantum yields [65]. On the basis of these principles, Forrest and co-workers [63] reported homoleptic iridium(III) carbene phosphorescent complex showing luminescence in the near-UV region with a relatively high quantum efficiency at room temperature. In addition, Cheng et al. [44] have recently reported iridium(III) carbene complexes that show wide-range color tuning from blue to red emitting. Using functional carbene groups as cyclometalated ligands brings a new and feasible way to construct wide energy-gap iridium(III) complex [46]. To date, however, iridium(III) complexes with carbene ligands showing blue or blue-green phosphorescence are rarely reported. Thus, further design and synthesis of novel carbene-based iridium(III) complexes will be helpful to investigate their structure-property relationship and develop more promising phosphorescent iridium(III) complexes for full-color display. Moreover, in numerous nitrogen heterocyclic ligands, 2-pyridylazole composed of the strong σ-donor property azole fragment together with the π-accepting ability pyridyl fragment, can enhance the chelate interaction and possess a very large intraligand π-π* energy gap. Furthermore, such ligands exhibit fascinating photoelectronic properties and can induce a blue-shifted emission, thereby they are regarded as the alternative chromophore for obtaining short-wavelength luminescent materials [4, 71, 72].

With the aim of obtaining efficient, stable and wide band gap phosphors, we herein designed and synthesized carbene-triazole based iridium(III) complexes

$(fpmi)_2Ir(mtzpy)$ (**1**) and **$(fpmi)_2Ir(phtzpy)$** (**2**) (**fpmi**: 1-(4-fluorophenyl)-3-methylimdazolin-2-ylidene-C,$C^{2'}$; **mtzpy**: 2-(5-methyl-2*H*-1,2,4-triazol-3-yl)pyridine; **phtzpy**: 2-(5-phenyl-2*H*-1,2,4-triazol-3-yl)pyridine; shown in Scheme 1). Their photophysical results indicate that both complexes exhibit strong greenish-blue emissions with quantum efficiencies of about 0.50 in CH_2Cl_2 solution. They also enjoy excellent electrochemical properties and thermal stabilities. Moreover, the theoretical calculations have been performed to gain insight into their photophysical and electrochemical properties. The vapor-deposited electroluminescence (EL) devices using complexes **1** and **2** as dopants have been fabricated successfully. The constructed greenish-blue and white OLEDs both exhibit good efficiencies. This result reveals that these two complexes offer an opportunity for constructing high performance OLEDs towards full-color displays.

2. Experimental

2.1 Materials and general information

All reactants and solvents employed in synthesis were commercially available without further purification. The solvents for characterization were purified or dried by standard methods. All of the reactions were carried out under a nitrogen atmosphere using standard Schlenk techniques in oil baths. ^{1}H NMR spectra were recorded at 25 ^{o}C in dry $CDCl_3$ or DMSO-d_6 on Bruker Avance 500 MHz with tetramethylsilane (TMS) as the internal standard. The molecular weights of complexes **1** and **2** were

recorded on Agilient 1100 LCMsD mass spectrometer. Elemental analyses (C, H and N) were performed on a Perkin-Elmer 240C elemental analyzer. UV-vis absorption spectra were recorded on a Hitachi U3030 spectrometer, and photoluminescence spectra were recorded using a F-7000 FL spectrophotometer. The excited-state lifetimes were measured on a transient spectrofluorimeter (Edinburgh FLS920) with a time-correlated single-photo-counting technique. The photoluminescence quantum yields (Φ_{PL}) in the degassed solution were determined by an integrating sphere (Edinburgh FLS920). Cyclic voltammetry (CV) was performed on a BAS 100 W instrument electrochemical analyzer at a scan rate of 100 mV s^{-1} in CH_2Cl_2 solutions of supporting electrolyte tetrabutylammonium hexafluorophosphate ((TBA)PF_6, 0.1 M). Glassy carbon electrode was used as the working electrode, an aqueous saturated calomel electrode as the reference electrode and a platinum wire as the counter electrode. Potentials were obtained using ferrocene-ferrocenium (Fc/Fc^+) couple as the internal standard. The solutions were deoxygenated with argon. Thermogravimetric analyses (TGA) were performed on a Perkin-Elmer TGA-2 thermogravimetric analyzer, with temperature gradient set at 10 °C min^{-1} from 55 °C to 800 °C under a flowing nitrogen atmosphere.

Insert **Scheme 1**

Scheme 1. Synthetic routes and structures of complexes **1** and **2**.

2.2 Synthesis

The carbene precursor 1-(4-fluorophenyl)-3-methyl-imidazolium iodide (**H_2fpmiI**) was prepared by reacting imidazole with 1-fluoro-4-iodobenzene using a modified Ullmann coupling reaction, following by N-methylation of the resulting N-arylimidazole with iodomethane [73] with a yield of 74%. The desired iridium(III) complexes were synthesized through a two-step reaction: firstly, the carbene precursor and iridium(III) trichoride hydrate were transformed into chloro-bridged iridium(III) dimers, following by adding a mixture of the ancillary ligand to give the desired heteroleptic iridium(III) complexes. In this paper the cyclometalated chloride-bridged dimer $[(fpmi)_2IrCl]_2$ was synthesized according to the described procedure by treating $IrCl_3 \cdot 3H_2O$ with silver(I) oxide and carbene precursor imidazolium iodide H_2fpmiI in refluent ethanol. The ancillary ligands 2-(5-methyl-2*H*-1,2,4-triazol-3-yl)pyridine (**Hmtzpy**) and 2-(5-phenyl-2*H*-1,2,4-triazol-3-yl)pyridine (**Hphtzpy**) were synthesized according to the literature [71, 74].

Synthesis of $[(fpmi)_2IrCl]_2$. A mixture of 1-(4-fluorophenyl)-3-methyl- imidazolium iodide (H_2fpmiI) (4.93 mmol, 1.50 g), silver(I) oxide (4.70 mmol, 1.09 g), iridium trichloride hydrate (2.35 mmol, 829 mg) in ethanol (70 mL) was heated to reflux under nitrogen atmosphere for 24 h in the dark. The reaction mixture was cooled to room temperature, and filtrated. The residue was washed with CH_2Cl_2. The filtrate was concentrated under reduced pressure and the resultant solid was purified by silica gel column chromatography using CH_2Cl_2 as eluent to give a grey white powder (18.4%). ^{1}H NMR (500MHz, $CDCl_3$, ppm): δ = 7.50 (s, *J* = 2 Hz, 4H), 7.11 (s, *J* = 2

Hz, 4H), 6.87 (dd, *J* = 5 Hz, *J* = 8.5 Hz, 4H), 6.40 (dd, *J* = 5.5 Hz, *J* = 8 Hz, 4H), 5.80 (dd, *J* = 2.5 Hz, *J* = 10 Hz, 4H), 3.87 (s, 12H). MS [m/z]: found 1157.1 (MH^+). Anal. Calcd. (%) for $C_{40}H_{32}N_8Cl_2F_4Ir_2$: C 41.52, H 2.77, N 9.69. Anal. found: C 41.57, H 2.80, N 9.70.

Synthesis of $(fpmi)_2Ir(mtzpy)$ (1). A mixture of $[(fpmi)_2IrCl]_2$ (0.10 mmol, 116 mg), 2-(5-methyl-2*H*-1,2,4-triazol-3-yl)pyridine (Hmtzpy) (0.22 mmol, 35 mg), and K_2CO_3 (0.22 mmol, 30 mg) in 2-ethoxyethanol (5.0 mL) was heated at 85°C under nitrogen atmosphere for 12 h. After cooled to room temperature, the reaction mixture was filtered. The residue was washed with methanol. The filtrate was concentrated under reduced pressure and the resultant solid was purified by silica gel column chromatography using acetone-ethyl acetate (2:1) as the eluent to yield a green-yellow solid (85.7%). ^{1}H NMR (500MHz, $CDCl_3$, ppm): δ = 8.10 (d, *J* = 7.5 Hz, 1H), 7.91 (d, *J* = 5.5 Hz, 1H), 7.72 (d, *J* = 7.5 Hz, 1H), 7.35 (dd, *J* = 1.5 Hz, *J* = 7 Hz, 2H), 7.26–6.97 (m, 3H), 6.83 (d, *J* = 1.5 Hz, 1H), 6.80 (d, *J* = 2 Hz, 1H), 6.62–6.53 (m, 2H), 6.12–6.04 (m, 2H), 3.14 (s, 3H), 2.95 (s, 3H), 2.45 (s, 3H). MS [m/z]: found 703.2 (MH^+). Anal. Calcd. (%) for $C_{28}H_{23}N_8F_2Ir$: C 47.85, H 3.28, N 15.95. Anal. Found: C 47.89, H 3.30, N 15.96.

Synthesis of $(fpmi)_2Ir(phtzpy)$ (2). The synthesis of complex **2** was similar to that of complex **1** except that the ancillary ligand 2-(5-methyl-2*H*-1,2,4-triazol -3-yl)pyridine (Hmtzpy) was placed with 2-(5-phenyl-2*H*-1,2,4-triazol-3-yl)pyridine (Hphtzpy).

Yield: 75.5%. ^{1}H NMR (500MHz, $CDCl_3$, ppm): δ = 8.23 (d, *J* = 8 Hz, 1H), 8.12 (d, *J* = 8 Hz, 2H), 7.95 (d, *J* = 5.5 Hz, 1H), 7.77 (t, *J* = 8 Hz, 1H), 7.37–7.33 (m, 4H), 7.06–7.00 (m, 4H), 6.83 (d, *J* = 2 Hz, 1H), 6.78 (d, *J* = 1.5 Hz, 1H), 6.62–6.59 (m, 2H), 6.18 (dd, *J* = 3 Hz, *J* = 8 Hz, 1H), 6.09 (dd, *J* = 2.5 Hz, *J* = 9.5 Hz, 1H), 3.16 (s, 3H), 2.99 (s, 3H). MS [m/z]: found 765.5 (MH^+). Anal. Calcd. (%) for $C_{33}H_{25}N_8F_2Ir$: C 51.80, H 3.27, N 14.65. Anal. Found: C 51.82, H 3.31, N 14.67.

2.3 Quantum chemical calculations

The ground and excited electronic states of these complexes were investigated by performing density functional theory (DFT) and time-dependent DFT (TD-DFT) calculations at PBE0 hybrid functional level [75]. Restricted and unrestricted formalisms were adopted on the ground-state and the lowest-lying triplet excited-state geometry optimizations, respectively. The "Double-ξ" quality basis sets were employed for the C, H, N and F atom (6-31G*) and the Ir atom (LanL2DZ). An effective core potential (ECP) replaces the inner core electrons of Ir leaving the outer core $(5s)^2(5p)^6$ electrons and the $(5d)^6$ valence electrons of Ir(III). The location of molecular orbitals such as the highest occupied molecular orbitals (HOMOs) and the lowest unoccupied molecular orbitals (LUMOs) were calculated at the ground states. TD-DFT calculations were performed based on the optimized structures at triplet states. Typically, the 10 triplet and singlet roots of the nonhermitian eigenvalue equations were obtained to determine the vertical excitation energies. Oscillator strengths were deduced from the dipole transition matrix elements. All calculations

reported here were performed with the Gaussian 09 software package [76].

2.4 EL device fabrication and characterization

Patterned indium-tin-oxide (ITO)-coated glass substrates with the sheet resistance of 20 Ω per square were subjected to a routine cleaning process with rinsing in Decon 90, deionized water, drying in an oven, and finally treating in a UV-ozone chamber. Organic layers and cathode were sequentially deposited on the ITO-glass substrates without breaking vacuum (~5.0×10^{-4} Pa). A shadow mask was used to define the cathode and to make four 10 mm^2 devices on each substrate. The thickness of the organic layers and metal were monitored in situ with quartz oscillator. Luminance-current-voltage characteristics of the unpackaged devices were measured simultaneously with a programmable Keithley 2400 source meter and a Minolta luminance meter LS-110. The spectra of the devices were measured with an Ocean Optics Maya 2000-PRO spectrometer. All the measurements were carried out at room temperature in air.

3. Results and Discussion

3.1 Synthesis and structural characterization

Scheme 1 shows the synthetic routes and structures of complexes **1** and **2**. The synthetic procedures are shown in Experimental Section. The complexes **1** and **2** were obtained from the reaction of the cyclometalated chloride-bridged dimer $[(fpmi)_2IrCl]_2$ with the ancillary ligand **Hmtzpy** and **Hphtzpy**, respectively, by a

bridge-splitting reaction. Then, the complexes were structurally characterized by ^{1}H NMR, mass spectrometry and elemental analysis (see Experimental Section).

3.2 Photophysical properties

UV-Vis absorption and photoluminescence (PL) spectra of complexes **1** and **2** in CH_2Cl_2 solution at room temperature are shown in Fig. 1. Both complexes possess similar absorption spectral features. The intense absorption bands in the spectral region of 260–290 nm (extinction coefficient $\varepsilon \approx 44000–50000\ M^{-1}\,cm^{-1}$) for **1** and 260–300 nm ($\varepsilon \approx 23000–30000\ M^{-1}\,cm^{-1}$) for **2**, respectively, are mainly assigned to the spin-allowed π–π* transition characteristic of the free ligands. While, the absorption bands at low energy from 300 nm extended to the visible region can be attributed to a combination of singlet and triplet metal-to-ligand charge transfer (MLCT) transitions, ligand-to-ligand charge transfer (LLCT) and spin-orbit coupling enhanced ^{3}π–π* transitions, which is similar to the previously reported works [67, 73]. Although complexes **1** and **2** have similar absorption band shapes, a bathochromic shifted absorption has been observed for complex **2** with respect to complex **1**. This can be rationalized by the additionally extended phenyl π-conjugation system in **2**, which extends the π orbital energy of the triazolate moiety [71]. The PL spectra in solution at room temperature (RT) and 77 K were also recorded and the corresponding data are summarized in Table 1. Upon photoexcitation at 282 nm, complexes **1** and **2** exhibit intense greenish-blue emission at 486 and 490 nm, respectively, as shown in Fig. 1. As for the PL spectrum of complex **2**, an approximately 4 nm red shift relative

to complex **1** is observed. With reference to the spectroscopic data of other similar iridium(III) complexes in the literature [44], complexes **1** and **2** probably possess the dominant ^{3}MLCT lowest-excited states rather than the ligand-centered (LC) $^3\pi$–π^* excited states due to their broad and structureless emission profiles at RT. The apparent rigidochromic shift and vibronic fine structures of the emission spectra at 77 K are detected (see Fig. S4, Supporting Information), further indicating that the excited-states characters of **1** and **2** are dominated by ^{3}MLCT transitions. This is also supported by the theoretical calculations (*vide infra*).

To further probe the photophysical properties, their Φ_{PL} in the degassed CH_2Cl_2 were measured at RT. For complex **1**, the Φ_{PL} is 0.51, together with the phosphorescence lifetimes (τ) of 130 ns. Meanwhile, the Φ_{PL} of complex 2 is 0.46 and the τ is 175 ns. These excited-state lifetimes on the order of microseconds are the signature of phosphorescence for iridium(III) complexes. Combining the equations $k_r = \Phi_{PL}/\tau$ and $k_{nr} = (1-\Phi_{PL})/\tau$, the radiative ($k_r$) and non-radiative ($k_{nr}$) decay rates can be calculated and the results are listed in Table 1. These two complexes show similar k_{nr} value, but the k_r value for **1** (3.9×10^6 s^{-1}) is obviously larger than that for **2** (2.6×10^6 s^{-1}), indicating that **1** would be more advantage of designing high efficient EL devices based on light-energy harvesting from the triplet excitons [77].

Insert **Fig. 1** and **Table 1**

Fig. 1. Absorption and photoluminescence spectra of complexes **1** and **2** in CH_2Cl_2 solution at RT.

Table 1. Selected photophysical and electrochemical properties of complexes **1** and **2**.

3.3 Electrochemical properties

The electrochemical behaviors of complexes **1** and **2** were investigated by cyclic voltammetry in CH_2Cl_2 solutions using ferrocenium/ferrocene (Fc/Fc^+) as the internal standard. The cyclic voltammograms are shown in Fig. S5 and the results are summarized in Table 1. During the anodic scan at the rate of 100 mV s^{-1}, both complexes exhibit reversible oxidation peaks with potentials in the region of 0.65–0.67 V, which could be assigned to the Ir^{III}/Ir^{IV} oxidation [78]. Indeed, this assumption is well supported by quantum chemical calculations. The HOMO energy level can be estimated from the measured onset oxidation potential. The onset oxidation potentials for complexes **1** and **2** are 0.48 and 0.53 V, respectively. Consequently, the corresponding HOMO levels are –5.28 eV for **1** and –5.33 eV for **2**. As discussed above, both complexes also exhibit similar absorption profiles. Hence, these results clearly suggest that their HOMO levels for them are almost identical, which locate on the carbene-based ligands and the iridium(III) core. On the basis of the spectroscopy data of absorption edge, the energy band gaps (E_g) of two complexes are calculated to be 2.98 and 2.93 eV, respectively. The calculated energy gaps demonstrate the complexes may be potentially suitable greenish-blue emitting materials. Complexes **1** and **2** display excellent electrochemical properties, which are beneficial for the application on OLEDs. The electrochemical properties indicate that

the two complexes display excellent electrochemical properties, which are beneficial for the application on OLEDs.

3.4 Quantum chemical calculations

To gain further insight into the photophysical and electrochemical behaviors, the quantum chemical calculations were performed. The selected molecular orbitals and orbital compositions that are mainly involved in the electronic ground states of the titled complexes were obtained from DFT calculations. The geometries of these complexes were fully optimized and exhibited a distorted octahedral geometry around the iridium(III) center. The HOMO and LUMO distributions are depicted in Fig. 2 and the important frontier orbital compositions for the involved orbitals are listed in Table S1. The lowest-lying triplet state for each complex is calculated by TD-DFT method and the results are summarized in Table S2.

Insert **Fig. 2**

Fig. 2. Calculated frontier molecular orbitals of complexes **1** and **2**.

DFT calculation results indicate that the LUMO of complex **1** almost coincides with that of complex **2**, which resides on the pyridine group and 1,2,4-triazol segment of ancillary ligand. It is noted that the methyl and phenyl groups in the ancillary ligand have no contribution to the LUMOs. Their HOMOs are mainly located on cyclometalated carbene ligands and d orbital of iridium(III) metal center. The

contributions of the different fragments (Ir, carbene ligand fpmi, mtzpy and phtzpy) in the HOMOs and LUMOs are similar for both complexes. The HOMOs have a strong weight on Ir and fpmi ligand (35.97%, 58.14% and 32.81%, 48.61% for complexes **1** and **2**, respectively), while LUMOs are essentially located on the ancillary ligand mtzpy or phtzty (>98% composition for both complexes). Their results are given in Table S1.

On the basis of the calculated phosphorescence of **1** and **2** in CH_2Cl_2 media, the lowest-lying triplet state (T_1) of complex **1** originates from the excitation of HOMO→LUMO (61%) and HOMO–1→LUMO (19%). As for complex **2**, the T_1 state originates from the excitation of HOMO→LUMO (80%). Accordingly, the T_1 states for both complexes have predominant characters of ^{3}MLCT (Ir atom to pyridine and 1,2,4-triazol groups of ancillary ligands) and ^{3}LLCT (cyclometalated carbene ligands fpmi to pyridine and 1,2,4-triazol groups of ancillary ligands) mixed with a small quantity of ^{3}ILCT (ancillary ligands to ancillary ligands) components (see table S2) This attribution can be found in some similar reports on carbene-based iridium(III) complexes [73, 79, 80]. The quantum chemical calculation results correlate well with the experimentally observed emission bands of two complexes.

3.5 Thermal analysis

The thermal properties of complexes **1** and **2** were investigated by thermo gravimetric analysis (TGA) under a flowing nitrogen atmosphere (see Fig. S6). The TGA curves show that, the decomposition temperatures (T_d) with a weight loss of 5% are 385 and

396 °C for complexes **1** and **2**, respectively, indicative of the good thermal stabilities. Noticeably, the T_d value of complex **2** is much higher than that of complex **1**, which may be due to the increased molecular sizes.

3.6 Phosphorescent OLED device

To evaluate their electroluminescent properties, complexes **1** and **2** were used as triplet emitters to fabricate **Device 1** and **Device 2** with the device configuration of ITO/MoO_3 (3 nm)/TAPC (30 nm)/TCTA (5 nm)/$Bepp_2$ (10 nm)/POAPF: **1** or **2** (10 wt%) (30 nm)/BPhen (35 nm)/LiF (0.5 nm)/Mg:Ag (120 nm), in which POAPF (2,7-bis(diphenylphosphoryl)-9-(4-diphenylamino)phenyl-9'-phenyl-fluorene) was used as the host material. Thin MoO_3 interlayer at the anode can enhance the hole injection into TAPC [81]. TAPC (1,1-bis(4-(N,N′-di(*p*-tolyl)amino)phenyl)cyclohexane) and TCTA (4,4′,4″-tris (carbazol-9-yl)-triphenylamine) serve as the hole injection and transporting layers, respectively. $Bepp_2$ (bis(2-(2-hydroxyphenyl)-pyridine) beryllium) is used as the spacer and used to improve excitons balance between hole and electron injection/transporting, while BPhen (4,7-diphenyl-1,10-phenanthroline) and LiF act as the electron transporting and injection layers, respectively (see Fig. 3).

Insert **Fig. 3**

Fig. 3. Device configuration and energy band diagram of the greenish-blue OLEDs, and the molecular structures of compounds used in the devices.

As shown in Fig. 4 (a), **Device 1** and **Device 2** present greenish-blue emission at 472 and 482 nm, respectively, and no additional emission signals from POAPF were observed, suggesting an efficient energy transfer from the host to the iridium(III) complexes. The CIE coordinates calculated from the EL spectra of **Device 1** and **Device 2** are (0.18, 0.29) and (0.20, 0.35), respectively. Moreover, as illustrated by the current density-voltage-brightness (*J*-*V*-*L*) characteristics in Fig. 4 (b), **Device 1** and **Device 2** show low turn-on voltage at about 3 V. At the practical brightnesses of 100 and 1000 cd m^{-2}, the driving voltages of these two devices still display low values varying from 4.6 to 7.4 V. **Device 1** reveals attractive performance with a maximum brightness (L_{max}) of 1956 cd m^{-2} at 9.8 V, a peak η_p of 11.43 lm W^{-1} and a maximum η_c of 11.78 cd A^{-1}, while for **Device 2**, L_{max} of 3206 cd m^{-2}, maximum η_c of 11.09 cd A^{-1} and maximum η_p of 8.40 lm W^{-1} are successfully achieved (data summarized in Table 2). Notably, these two devices still remain relatively high efficiencies of 6.08, 1.60 lm W^{-1} for **Device 1** and 7.15, 3.06 lm W^{-1} for **Device 2** at 100 and 1000 cd m^{-2}, respectively. Such efficient EL performances, especially the low driving voltages at a high brightness level make these complexes beneficial for the application on flat-panel display and lighting source.

Fig. 4. (a) EL spectra of the greenish-blue devices at 7 V; (b) *J*-*V*-*L* characteristics for **Device 1** and **Device 2**; (c) η_p-*L*-η_c characteristics for the **Device 1**; (d) η_p-*L*-η_c characteristics for the **Device 2**.

Insert **Table 2**

Table 2. Summary of device performances.

Moreover, encouraged by the successful development of the greenish-blue OLEDs, we tried to fabricate white OLEDs using **1** to combine with one orange phosphor **$(pbi)_2Ir(biq)$** synthesized in our group [82]. The resulting white OLED **W1** has a configuration of ITO/MoO_3 (3 nm)/TAPC (30 nm)/TCTA (5 nm)/POAPF: orange emitter (7 wt%) (5 nm)/POAPF: **1 (**10 wt%) (25 nm)/BPhen (35 nm)/LiF (0.5 nm)/Mg:Ag (120 nm). The general structure for **W1** is shown in Fig. 5 (a). It can be found from Fig. 5 (b) that, the EL spectra contain two main bands located at 478 and 578 nm , which are ascribed to the emission from complex **1** and the orange emitter, respectively. The obtained CIE coordinates for this white OLED are (0.34, 0.40), which closes to ideal white light with the CIE coordinates of (0.33, 0.33). As depicted in Fig. 5 (c), the **W1** displays a low turn-on voltage of 2.71 V and a maximum brightness of 3910 cd m^{-2} at 8.6 V. An excellent performance with a maximum η_c of 10.81 cd A^{-1}, and a peak η_p of 9.95 lm W^{-1} was obtained for this device. At a high luminance of 1000 cd m^{-2}, the two element **W1** retained a favorable η_c of 7.61 cd A^{-1} and a η_p of 4.17 lm W^{-1}. These results indicate the two iridium(III) complexes are appropriate phosphorescent dyes to fabricate efficient-performance white device. As such, future studies will focus on device optimization of the doping concentration and layer thickness to further improve the performance of greenish-blue and white

devices.

Insert **Fig. 5**

Fig. 5. (a) The general structure and (b) EL spectra at 7 V of the two-element **W1**; (c) *J-V-L* and (d) η_p-*L*-η_c characteristics for the **W1**.

4. Conclusions

In summary, two new iridium(III) complexes based on high-field strength carbene cyclometalated ligands and triazole-pyridine type ligand were designed and synthesized. Both complexes show intense greenish-blue emission with quantum efficiencies of ~0.50, excellent electrochemical as well as good thermal properties. The theoretical calculations have also been performed to ascertain the nature of their excited-states characters and rationalize the photophysical and electrochemical properties. In addition, the use of these two complexes as dopant, greenish-blue phosphorescent OLEDs have been successfully achieved, exhibiting high efficiencies of 11.78 cd A^{-1} and 11.43 lm W^{-1} for **Device 1**, and good values of 11.09 cd A^{-1} and 8.40 lm W^{-1} for **Device 2**. Profiting from these favourable EL properties, a white device utilizing **1** and an orange phosphor **$(pbi)_2Ir(biq)$** was fabricated, showing η_c of 10.81 cd A^{-1} and η_p of 9.95 lm W^{-1} with $CIE_{x,y}$ values of (0.34, 0.40). The pronounced results obtained in this work indicate that complexes **1** and **2** provide an opportunity for constructing good performance OLEDs towards full-color displays.

Acknowledgements

The authors gratefully acknowledge the financial support from NSFC (21273030, 21303012, 51203017, 21203019, 21131001 and 60937001), 973 Program (2009CB623605), the Science and Technology Development Planning of Jilin Province (20130522167JH and 20130204025GX) and the Fundamental Research Funds for the Central Universities (12QNJJ012).

References

[1] M. A. Baldo, S. Lamansky, P. E. Burrows, M. E. Thompson, S. R. Forrest. Appl. Phys. Lett. 75 (1999) 4-6.

[2] S. Reineke, F. Lindner, G. Schwartz, N. Seidler, K. Walzer, B. Lüssem, K. Leo. Nature 459 (2009) 234-238.

[3] L. Wang, Y. Jiang, J. Luo, Y. Zhou, J. Zhou, J. Wang, J. Pei, Y. Cao. Adv. Mater. 21 (2009) 4854-4858.

[4] Y. Chi, P. T. Chou. Chem. Soc. Rev. 39 (2010) 638-655.

[5] C. Ulbricht, B. Beyer, C. Friebe, A. Winter, U. S. Schubert. Adv. Mater. 21 (2009) 4418-4441.

[6] J. I. Goldsmith, W. R. Hudson, M. S. Lowry, T. H. Anderson, S. Bernhard. J. Am. Chem. Soc. 127 (2005) 7502-7510.

[7] Y. J. Yuan, Z. T. Yu, X. Y. Chen, J. Y. Zhang, Z.G. Zou. Chem. Eur. J. 17 (2011) 12891-12895.

[8] M. A. Baldo, D. F. O'Brien, Y. You, A. Shoustikov, S. Sibley, M. E. Thompson, S. R. Forrest. Nature 395 (1998) 151-154.

[9] Y. Ma, H. Zhang, J. Shen, C. Che. Synthetic Met. 94 (1998) 245-248.

[10] R. D. Costa, E. Ortí, H. J. Bolink, F. Monti, G. Accorsi, N. Armaroli. Angew. Chem. Int. Ed. 51 (2012) 8178-8211.

[11] L. J. Soltzberg, J. D. Slinker, S. Flores-Torres, D. A. Bemards, G. G. Malliaras, H. D. Abruña, J. S. Kim, R. H. Friend, M. D. Kaplan, V. Goldberg. J. Am. Chem. Soc. 128 (2006) 7761-7764.

[12] S. Fantacci, F. De Angelis. Coord. Chem. Rev. 255 (2011) 2704-2726.

[13] B. Happ, A. Winter, M. D. Hager, U. S. Schubert. Chem. Soc. Rev. 41 (2012) 2222-2255.

[14] B. Carlson, G. D. Phelan, J. H. Kim, A. K.-Y. Jen, L. Dalton. MRS Proceedings 771 (2003) 363-368.

[15] B. S. Du, J. L. Liao, M. H. Huang, C. H. Lin, H. W. Lin, Y. Chi, H. A. Pan, G. L. Fan, K. T. Wong, G. H. Lee, P. T. Chou. Adv. Funct. Mater. 22 (2012) 3491-3499.

[16] L. Zhang, B. Li, Z. Su. J. Phys. Chem. C. 113 (2009) 13968-13973.

[17] Q. Zhang, J. Ding, Y. Cheng, L. Wang, Z. Xie, X. Jing, F. Wang. Adv. Funct. Mater. 17 (2007) 2983-2990.

[18] L. Xiao, Z. Chen, B. Qu, J. Luo, S. Kong, Q Gong, J. Kido. Adv. Mater. 23 (2011) 926-952.

[19] R. Czerwieniec, J. Yu, H. Yersin. Inorg. Chem. 50 (2011) 8293-8301.

[20] G. Zhou, Q. Wang, X. Wang, C. L. Ho, W. Y. Wong, D. Ma, L. Wang, Z. Lin. J. Mater. Chem. 20 (2010) 7472-7484.

[21] C. H. Chen, F. I. Wu, Y. Y. Tsai, C. H. Cheng. Adv. Funct. Mater. 21 (2011)

3150-3158.

[22] Y. Wu, S. X. Wu, H. B. Li, Y. Geng, Z. M. Su. Dalton Trans. 40 (2011) 4480-4488.

[23] C. M. Che, S. C. Chan, H. F. Xiang, M. C. W. Chan, Y. Liu, Y. Wang. Chem. Commum. (2004) 1484-1485.

[24] Z. He, W. Y. Wong, X. Yu, H. S. Kwok, Z. Lin. Inorg. Chem. 45 (2006) 10922-10937.

[25] G. J. Zhou, W. Y. Wong, B. Yao, Z. Xie, L. Wang. J. Mater. Chem. 18 (2008) 1799-1809.

[26] G. Zhou, Q. Wang, C. L. Ho, W. Y. Wong, D. Ma, L. Wang. Chem. Commun. (2009) 3574-3576.

[27] G. Zhou, W. Y. Wong, X. Yang. Chem. Asian J. 6 (2011) 1706-1727.

[28] X. N. Li, Z. J. Wu, X. Y. Li, H. J. Zhang, X. J. Liu. J. Comput. Chem. 32 (2011) 1033-1042.

[29] Z. Q. Chen, Z. Q. Bian, C. H. Huang. Adv. Mater. 22 (2010) 1534-1539.

[30] L. He, J. Qiao, L. Duan, G. Dong, D. Zhang, L. Wang, Y. Qiu. Adv. Funct. Mater. 19 (2009) 2950-2960.

[31] Y. You, W. Nam. Chem. Soc. Rev. 41 (2012) 7061-7084.

[32] A. Tsuboyama, H. Iwawaki, M. Furugori, T. Mukaide, J. Kamatani, S. Igawa, T. Moriyama, S. Miura, T. Takiguchi, S. Okada, M. Hoshino, K. Ueno. J. Am. Chem. Soc. 125 (2003) 12971-12979.

[33] Q. Mei, L. Wang, B. Tian, B. Tong, J. Wen, B. Zhang, Y. Jiang, W. Huang. Dyes

Pigments 97 (2013) 43-51.

[34] Y. You, S. Y. Park. Dalton Trans. (2009) 1267-1282.

[35] J. Zou, H. Wu, C. S. Lam, C. Wang, J. Zhu, C. Zhong, S. Hu, C. L. Ho, G. J. Zhou, H, Wu, W. C. H. Choy, J. Peng, Y.Cao, W. Y. Wong. Adv. Mater. 23 (2011) 2976-2980.

[36] B. Zhang, G. Tan, C. S. Lam, B. Yao, C. L. Ho, L. Liu, Z. Xie, W. Y. Wong, J. Ding, L. Wang. Adv. Mater. 24 (2012) 1873-1877.

[37] W. Y. Wong, C. L. Ho. Coord. Chem. Rev. 253 (2009) 1709-1758.

[38] W. Y. Wong, C. L. Ho. J. Mater. Chem. 19 (2009) 4457-4482.

[39] G. Zhou, W. Y. Wong, S. Suo. J. Photochem. Photobio. C: Photochem. Rev. 11 (2010) 133-156.

[40] C. L. Ho, W. Y. Wong. Coord. Chem. Rev. 257 (2013) 1614-1649.

[41] Y. Kawamura, K. Goushi, J. Brooks, J. J. Brown, H. Sasabe, C. Adachi. Appl. Phys. Lett. 86 (2005) 071104-1-071104-3.

[42] B. Liang, C. Y. Jiang, Z. Chen, X. J. Zhang, H. H. Shi, Y. Cao. J. Mater. Chem. 16 (2006) 1281-1286.

[43] H. Sasabe, T. Chiba, S. J. Su, Y. J. Pu, K. Nakayama, J. Kido. Chem. Commun. (2008) 5821-5823.

[44] K. Y. Lu, H. H. Chou, C. H. Hsieh, Y. H. Ou Yang, H. R. Tsai, H. Y. Tsai, L. C. Hsu, C. Y. Chen, I. C. Chen, C. H. Cheng. Adv. Mater. 23 (2011) 4933-4937.

[45] H. Sasabe, J. Kido. Chem. Mater. 23 (2011) 621-630.

[46] K. S. Yook, J. Y. Lee. Adv. Mater. 24 (2012) 3169-3190.

[47] H. Fu, Y. M. Cheng, P. T. Chou, Y. Chi. Mater. today 14 (2011) 472-479.

[48] C. L. Ho, W. Y. Wong. New. J. Chem. 37 (2013) 1665-1683.

[49] G. Zhou, C. L. Ho, W. Y. Wong, Q. Wang, D. Ma, L. Wang, Z. Lin, T. B. Marder, A. Beeby. Adv. Funct. Mater. 18 (2008) 499-511.

[50] C. L. Ho, Q. Wang, C. S. Lam, W. Y. Wong, D. Ma, L. Wang, Z. Q. Gao, C. H. Chen, K. W. Cheah, Z. Lin. Chem. Asian J. 4 (2009) 89-103.

[51] S. J. Yun, H. J. Seo, M. Song, S. H. Jin, S. K. Kang, Y. I. Kim. J. Organomet. Chem. 724 (2013) 244-250.

[52] M. Xu, R. Zhou, G. Wang, Q. Xiao, W. Du, G. Che. Inorganica Chimica Acta 361 (2008) 2407-2412.

[53] R. Ragni, E. A. Plummer, K. Brunner, J. W. Hofstraat, F. Babudri, G. M. Farinola, F. Naso, L. De Cola. J. Mater. Chem. 16 (2006) 1161-1170.

[54] S. J. Lee, K. M. Park, K. Yang, Y. Kang. Inorg. Chem. 48 (2009) 1030-1037.

[55] L. L. Wu, C. H. Yang, I. W. Sun, S. Y. Chu, P. C. Kao, H. H. Huang. Organometallics 26 (2007) 2017-2023.

[56] D. Di Censo, S. Fantacci, F. De Angelis, C. Klein, N. Evans, K, Kalyanasundaram, H. J. Bolink, M. Gratzel, M. K. Nazeeruddin. Inorg. Chem. 47 (2008) 980-989.

[57] A. B. Tamayo, B. D. Alleyne, P. I. Djurovich, S. Lamansky, I. Tsyba, N. N. Ho, R. Bau, M. E. Thompson. J. Am. Chem. Soc. 125 (2003) 7377-7387.

[58] S. C. Lo, C. P. Shipley, R. N. Bera, R. E. Harding, A. R. Cowley, P. L. Burn, I. D. W. Samuel. Chem. Mater. 18 (2006) 5119-5129.

[59] F. E. Hahn, M. C. Jahnke. Angew. Chem. Int. Ed. 47 (2008) 3122-3172.

[60] G. C. Fortman, S. P. Nolan. Chem. Soc. Rev. 40 (2011) 5151-5169.

[61] N. Darmawan, C. H. Yang, M. Mauro, M. Raynal, S. Heun, J. Pan, H. Buchholz, P. Braunstein, L. De Cola. Inorg. Chem. 52 (2013) 10756-10765.

[62] V. K. Au , K. M. Wong, N. Zhu,V. W. Yam. J. Am. Chem. Soc. 131 (2009) 9076-9085.

[63] T. Sajoto, P. I. Djurovich, A. Tamayo, M. Yousufuddin, R. Bau, M. E. Thompson, R. J. Holmes, S. R. Forrest. Inorg. Chem. 44 (2005) 7992-8003.

[64] S. Haneder, E. Da Como, J. Feldmann, J. M. Lupton, C. Lennartz, P. Erk, E. Fuchs, O. Molt, I. Münster, C. Schildknecht, G. Wagenblast. Adv. Mater. 20 (2008) 3325-3330.

[65] Y.C. Chiu, J. Y. Huang, Y. Chi, C. C. Chen, C. H. Chang, C. C. Wu, Y. M. Cheng, Y. C. Yu, G. H. Lee, P. T. Chou. Adv. Mater. 21 (2009) 2221-2225.

[66] Z. M. Hudson, C. Sun, M. G. Helander, Y. L. Chang, Z. H. Lu, S. N. Wang. J. Am. Chem. Soc. 134 (2012) 13930-13933.

[67] C. H. Yang, J. Beltran, V. Lemaur, J. Cornil, D. Hartmann, W. Sarfert, R. Fröhlich, C. Bizzarri, L. De Cola. Inorg. Chem. 48 (2010) 9891-9901.

[68] R. J. Holmes, S. R. Forrest, T. Sajoto, A. Tamayo, P. I. Djurovich, M. E. Thompson, J. Brooks, Y. J. Tung, B. W. D'Andrade, M. S. Weaver, R. C. Kwong, J. J. Brown. Appl. Phys. Lett. 87 (2005) 243507-1-243507-3.

[69] C. F. Chang, Y. M. Cheng, Y. Chi, Y. C. Chiu, C. C. Lin, G. H. Lee, P. T. Chou, C. C. Chen, C. H. Chang, C. C. Wu. Angew. Chem. Int. Ed. 47 (2008) 4542-4545.

[70] H. Sasabe, J. I. Takamatsu, T. Motoyama, S. Watanabe, G. Wagenblast, N. Langer, O. Molt, E. Fuchs, C. Lennartz, J. Kido. Adv. Mater. 22 (2010) 5003-5007.

[71] E. Orselli, G. S. Kottas, A. E. Konradsson, P. Coppo, R. Fröhlich R, L. De Cola, A. Van Dijken, M. Büchel, H. Börner. Inorg. Chem. 46 (2007) 11082-11093.

[72] B. Liang, S. Hu, Y. Liu, Z. Fan, X. Wang, W. Zhu, H. Wu, Y. Cao. Dyes Pigments 99 (2013) 41-51.

[73] C. H. Hsieh, F. I. Wu, M. J. Huang, K. Y. Liu, P. Y. Chou, Y. H. Yang, S. H. Wu, I. C. Chen, S. H. Chou, K. T. Wong, C. H. Cheng. Chem. Eur. J. 17 (2011) 9180-9187.

[74] G. G. Shan, H. B. Li, D. X. Zhu, Z. M. Su, Y. Liao. J. Mater. Chem. 22 (2012) 12736-12744.

[75] C. Adamo, V. Barone. J. Chem. Phys. 110 (1999) 6158-6170.

[76] M. J. Frisch, G. W. Trucks, H. B. Schlegel, G. E. Scuseria, M. A. Robb, J. R. Cheeseman, G. Scalmani, V. Barone, B. Mennucci, G. A. Petersson, H. Nakatsuji, M. Caricato, X. Li, H. P. Hratchian, A. F. Izmaylov, J. Bloino, G. Zheng, J. L. Sonnenberg, M. Hada, M. Ehara, K. Toyota, R. Fukuda, J. Hasegawa, M. Ishida, T. Nakajima, Y. Honda, O. Kitao, H. Nakai, T. Vreven, J. A. Montgomery, Jr., J. E. Peralta, F. Ogliaro, M. Bearpark, J. J. Heyd, E. Brothers, K. N. Kudin, V. N. Staroverov, R. Kobayashi, J. Normand, K. Raghavachari, A. Rendell, J. C. Burant, S. S. Iyengar, J. Tomasi, M. Cossi, N. Rega, J. M. Millam, M. Klene, J. E. Knox, J. B. Cross, V. Bakken, C. Adamo, J. Jaramillo, R. Gomperts, R. E. Stratmann, O. Yazyev, A. J. Austin, R. Cammi, C. Pomelli, J. W. Ochterski, R. L. Martin, K. Morokuma, V. G. Zakrzewski, G. A. Voth, P. Salvador, J. J. Dannenberg, S. Dapprich, A. D. Daniels, O. Farkas, J. B.

Foresman, J. V. Ortiz, J. Cioslowski, D. J. Fox, Gaussian 09, Revision A.02; Gaussian Inc.: Wallingford CT, 2009.

[77] W. Y. Wong, G. J. Zhou, X. M. Yu, H. S. Kwok, B. Z. Tang. Adv. Funct. Mater. 16 (2006) 838-846.

[78] L. J. Deng, T. Zhang, R. J. Wang, J. Y. Li. J. Mater. Chem. 22 (2012) 15910-15918.

[79] Z. F. Xie, F. Q. Bai, J. Wang, H. X. Zhang. Mol. phys. 109 (2011) 1657-1675.

[80] Y. C. Liu, X. B. Sun, G. Gahungu, X. C. Qu, Y. Wang, Z. J. Wu. J. Mater. Chem.C 1 (2013) 3700-3709.

[81] M. Kröger, S. Hamwi, J. Meyer, T. Riedl, W. Kowalsky, A. Kahn. Appl. Phys. Lett. 95 (2009) 123301-1-123301-3.

[82] H. Cao, G. Shan, X. Wen, H. Sun, Z. Su, R. Zhong, W. Xie, P. Li, D. Zhu. J.Mater.Chem. 1 (2013) 7371-7379.

Table 1. Selected photophysical and electrochemical properties of complexes **1** and **2**.

Table 2. Summary of device performances.

Table 1. Selected photophysical and electrochemical properties of complexes **1** and **2**.

complex	Absorption λ [nm][a] (ε, $10^4 M^{-1}cm^{-1}$)	PL RT λ_{max} [nm][a]	PL 77 K λ_{max} [nm][a]	Φ_{PL}[a]	τ [ns][a]	k_r [$10^6 s^{-1}$][b]	k_{nr} [$10^6 s^{-1}$][b]	E_{ox}^{onset} [V][c]	E_g [eV][d]	HOMO [eV][e]	LUMO [eV][f]
1	275(4.99), 342(1.11), 395(0.21)	474, 486	458, 483	0.51	130	3.9	3.8	0.48	2.98	–5.28	–2.30
2	280(2.97), 347(0.51), 405(0.05)	480, 490	465, 489	0.46	175	2.6	3.1	0.53	2.93	–5.33	–2.40

[a] Measured in CH_2Cl_2 solution with concentration = 2.5×10^{-5} M at RT; [b] k_r and k_{nr} were calculated according to the equation, $k_r = \Phi_{PL}/\tau$ and $k_{nr} = (1-\Phi_{PL})/\tau$; [c] Onset oxidation potentials measured by cyclic voltammetry using Fc/Fc^+ as the internal reference in CH_2Cl_2; [d] E_g estimated from the UV-vis absorption spectra edge; [e] HOMO = $-4.8-E_{ox}^{onset}$ eV; [f] LUMO = HOMO + E_g.

Table 2. Summary of device performances.

Device	V_{on} [V][a]	L_{max} [cd m^{-2}], [V]	η_c [cd A^{-1}][b]	η_p [lm W^{-1}][c]	λ_{max} at 7 V [nm]	CIE at 7 V
Device 1	3.06	1956, 9.8	11.78/9.35/3.79	11.43/6.08/1.60	472	(0.18, 0.29)
Device 2	3.02	3206, 9.6	11.09/10.61/6.56	8.40/7.15/3.06	482	(0.20, 0.35)
W1	2.71	3910, 8.6	10.81/10.64/7.61	9.95/8.18/4.17	478/578	(0.34, 0.40)

[a] V_{on} is the turn-on voltage measured at 1 cd m^{-2}.

[b] η_c is the current efficiency recorded at max, 100, 1000 cd m^{-2}.

[c] η_p is the power efficiency recorded at max, 100, 1000 cd m^{-2}.

Captions of Figures

Scheme 1. Synthetic routes and structures of complexes **1** and **2**.

Fig. 1. Absorption and photoluminescence spectra of complexes **1** and **2** in CH_2Cl_2 solution at RT.

Fig. 2. Calculated frontier molecular orbitals of complexes **1** and **2**.

Fig. 3. Device configuration and energy band diagram of the greenish-blue OLEDs, and the molecular structures of compounds used in the devices.

Fig. 4. (a) EL spectra of the greenish-blue devices at 7 V; (b) *J*-*V*-*L* characteristics for **Device 1** and **Device 2**; (c) η_p-*L*-η_c characteristics for the **Device 1**; (d) η_p-*L*-η_c characteristics for the **Device 2**.

Fig. 5. (a) The general structure and (b) EL spectra at 7 V of the two-element **W1**; (c) *J*-*V*-*L* and (d) η_p-*L*-η_c characteristics for the **W1**.

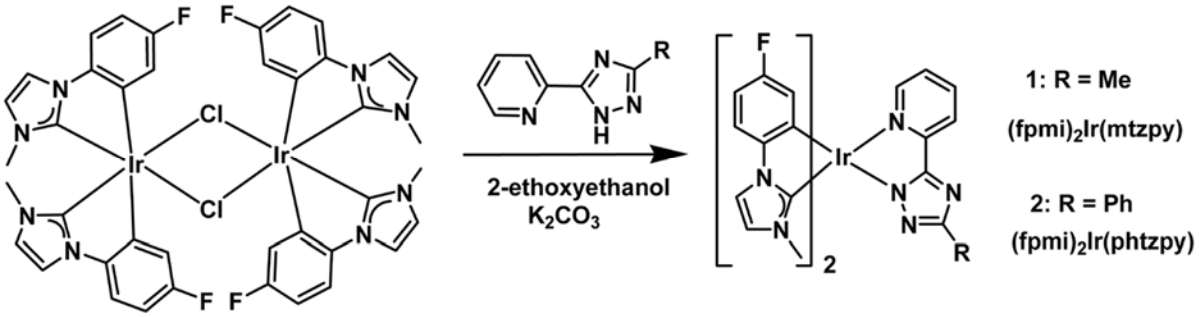

Scheme 1. Synthetic routes and structures of complexes **1** and **2**.

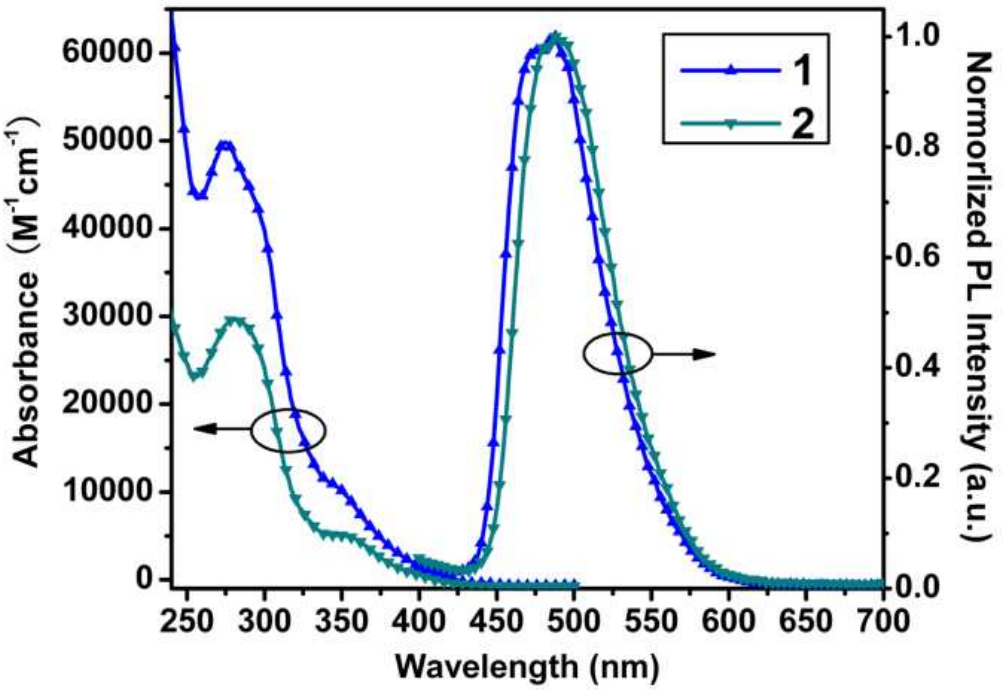

Fig. 1. Absorption and photoluminescence spectra of complexes **1** and **2** in CH_2Cl_2 solution at RT.

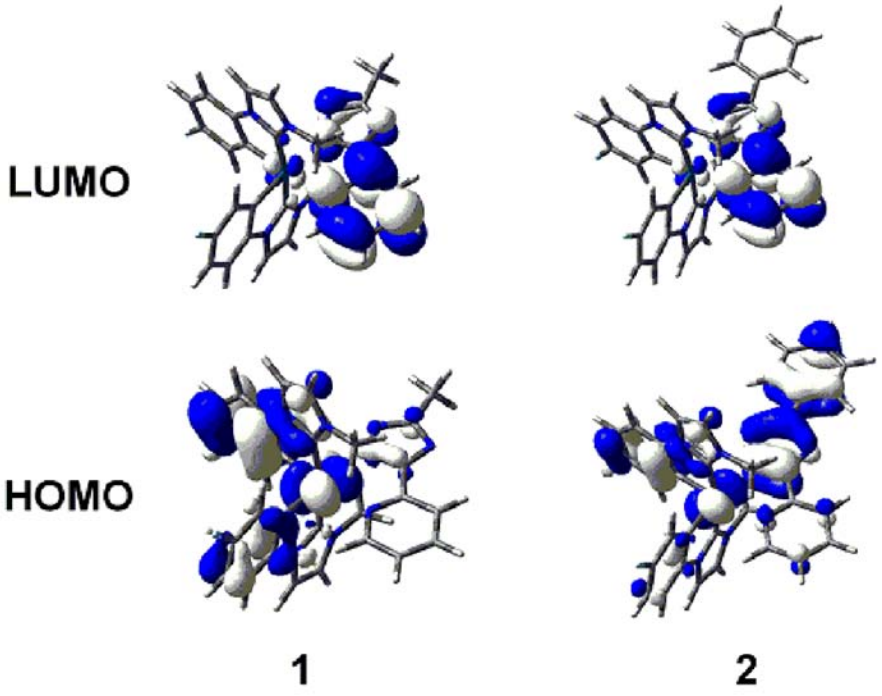

Fig. 2. Calculated frontier molecular orbitals of complexes **1** and **2**.

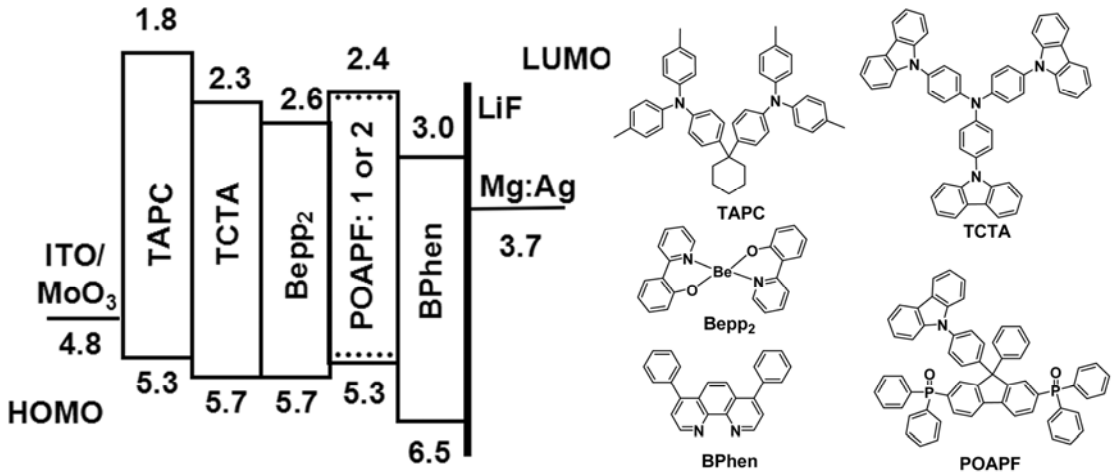

Fig. 3. Device configuration and energy band diagram of the greenish-blue OLEDs, and the molecular structures of compounds used in the devices.

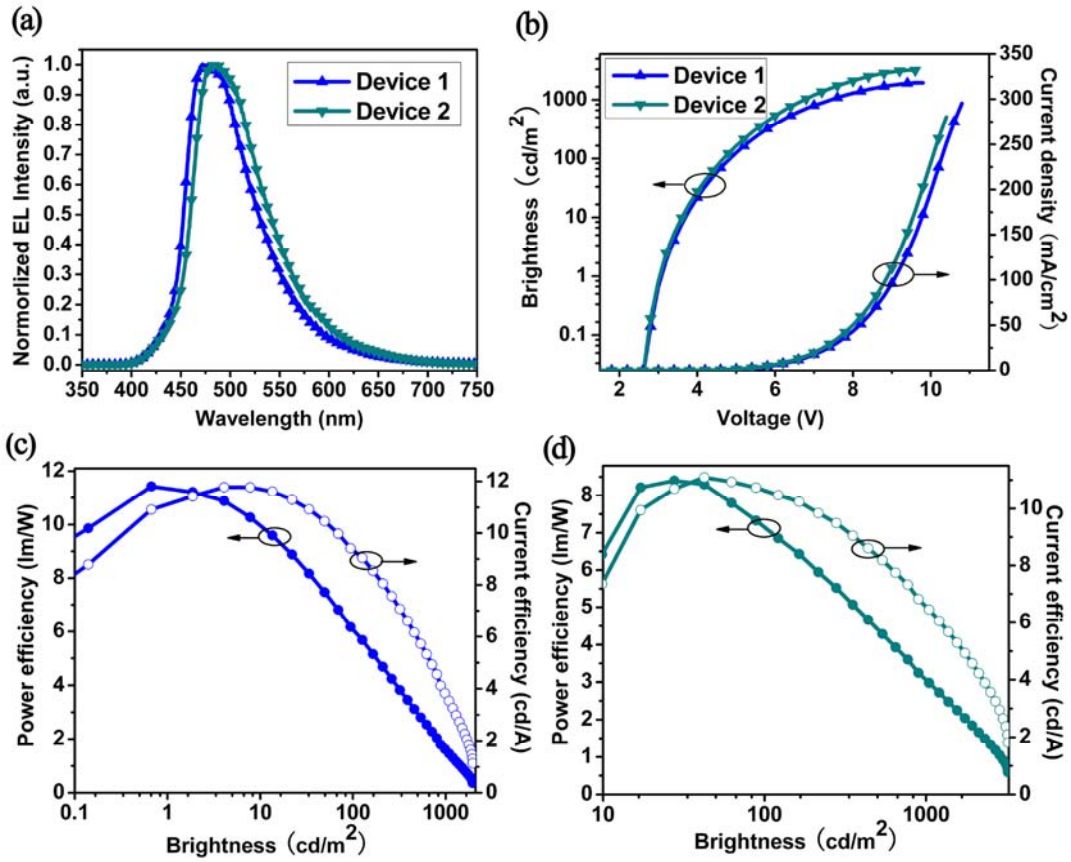

Fig. 4. (a) EL spectra of the greenish-blue devices at 7 V; (b) *J-V-L* characteristics for **Device 1** and **Device 2**; (c) η_p-*L*-η_c characteristics for the **Device 1**; (d) η_p-*L*-η_c characteristics for the **Device 2**.

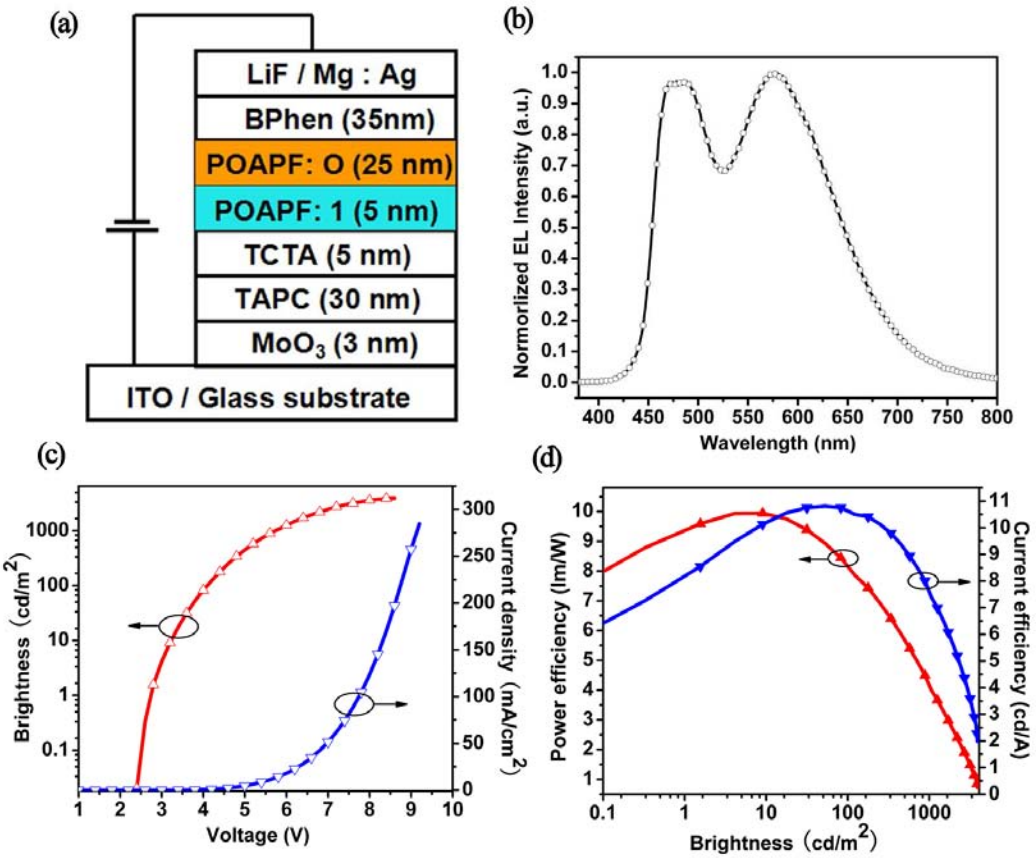

Fig. 5. (a) The general structure and (b) EL spectra at 7 V of the two-element **W1**; (c) *J*-*V*-*L* and (d) η_p-*L*-η_c characteristics for the **W1**.

Highlights

► Two Ir(III) complexes with carbene ligands are designed and synthesized.

►Both complexes exhibit greenish-blue emission with high efficiency of ~0.5.

►The experimental results are rationalized by the theoretical calculations.

►Greenish-blue OLEDs show good efficiencies of 11.78 cd A^{-1} and 11.43 lm W^{-1}.

►A white OLED using one of them as dopant is successfully fabricated.